

## **Supplementary Data File 1: Immunohistochemistry Methods**

### **1. Myenteric Plexus**

#### *1.1. Tissues*

Full thickness tissue, approximately 1 x 1 cm, were fixed for a minimum of 24 h in 10 % neutral buffered formal saline solution (Sigma-Aldrich Co. LLC) before transferring to 70 % ethanol (Sigma-Aldrich Co. LLC). The samples were then processed and embedded in paraffin blocks according to standard operating procedures.

Multiple 4  $\mu\text{m}$  sections were cut from each paraffin-embedded tissue using a rotatory microtome (Thermo Fisher Scientific). The sections were floated out on a warm water bath to remove creases and picked up on positively charged glass slides (VWR, Int). The sections were then dried overnight in a 37°C oven.

The block was trimmed and a section was prepared from each block for hematoxylin & eosin staining before further sets of sections were cut and stained for anti-protein gene product 9.5 (anti-PGP9.5), anti-human neuronal protein C/D (anti-HuC/D), anti-choline acetyltransferase (anti-ChAT) and anti-neuronal nitric oxide synthase (anti-nNOS). In the block from each patient, and for each antibody, the different sections used were at least 16  $\mu\text{m}$  apart from each other. Sections were dewaxed and dehydrated through a series of xylenes and industrial methylated spirits (VWR, Int). Antigen retrieval was then carried out according to the antibody being used (Suppl. Table 1).

**Supplementary Table 1: Antibodies used**

Primary antibody	Supplier (code)	Species raised in	Clonality	Antigen Retrieval		Dilution	Incubation Period	Detection method	Secondary antibodies	Visualization method
				Method	Buffer					
anti-PGP9.5	AbD Serotec (7863-0504)	rabbit	polyclonal	DAKO PT Link system (factory settings)	High pH	1:4000	30 min	DAKO EnVision™ FLEX+, High pH	EnVision™ FLEX+ Rabbit	EnVision™ FLEX DAB+ Substrate Chromogen System
anti-HuC/D	Life technologies (1600899)	mouse	monoclonal	DAKO PT Link system (factory settings)	High pH	1:100	30 min	DAKO EnVision™ FLEX+, High pH	EnVision™ FLEX+ Mouse (LINKER)	EnVision™ FLEX DAB+ Substrate Chromogen System
anti-ChAT	Millipore (AB144P)	goat	polyclonal	Microwave -25 min	pH 6.0	1:50	60 min	Vectastain® Universal elite	Horse anti goat (1:250)	Dako Liquid DAB+ Substrate Chromogen System
anti-nNOS-(neuron)-c-terminal	Abcam (ab72428)	goat	polyclonal	Microwave 35 min	pH 9.0	1:300	40 min	Vectastain® Universal elite	Horse anti goat (1:250)	Dako Liquid DAB+ Substrate Chromogen System

**KEY:** **PGP9.5:** protein gene product 9.5; **HuC/D:** human neuronal proteins HuC and HuD; **ChAT:** choline acetyltransferase; **nNOS:** neuronal nitric oxide synthase.

Two visualization methods were used depending on the primary antibodies: the DAKO EnVision™ FLEX+, High pH (DAKO, K-8012) visualization system; and the Vectastain Universal elite ABC RTU Kit (Vector Laboratories). Both methods were performed using the Dako Autostainer Instruments.

1. Dako Envision™ FLEX+ method

Following heat-induced epitope retrieval using the PT-Link system, endogenous peroxidase was blocked with EnVision™ FLEX Peroxidase-Blocking Reagent (DM821). Primary antibodies were applied, followed by the appropriate secondary antibodies [EnVision™ FLEX+ Rabbit or EnVision™ FLEX+ Mouse (LINKER)] and Dako EnVision™ FLEX /HRP detection reagent. The concentrated diaminobenzidine (DAB) substrate solution [EnVision™ FLEX DAB+ Chromogen (DM827)] and EnVision™ FLEX Substrate Buffer (DM823) were then added. Samples were washed with Wash Buffer (20x) between each staining step.

2. Vectastain® Universal elite method

Following antigen retrieval, endogenous peroxidase blocking solution and normal horse blocking serum from the Vectastain® Elite R.T.U. kit were applied depending on the requirement of the primary antibodies. Primary antibodies were then added before the universal biotinylated secondary antibody (horse anti-goat IgG) was added. The sections were then incubated with Vectastain Elite ABC reagent (Reagent A: Avidin DH solution; and Reagent B: biotinylated enzyme) followed by DAB Chromogen and substrate Buffer from the Biogenex Two Component DAB kit. Samples were washed with Wash Buffer (20x) between each staining step.

Following visualization, cell nuclei were counterstained with hematoxylin using the Gemini immune program on the Shandon Varistain Gemini machine, before sealing with coverslips. To validate staining and check for non-specific binding and false positive results, positive and negative (no primary) controls were performed in normal colon (for anti-PGP 9.5; anti-HuB/C/D, anti-nNOS) and spinal cord (for anti-ChAT), with or without the primary antibodies respectively.

Stained slides were scanned with the Nanozoomer 2.0-HT digital slide scanner: C9600 (Hamamatsu) and saved onto a hard drive. Digital slides were then visualized and assessed using the NDP.view2 Viewing software: U12388-01 (Hamamatsu) projected on to a screen from a distance of 36 m (NEC multimedia projector NP-M260X, resolution: 1024 x 768, contrast ratio: 2000:1).

## 1.2. *Counting myenteric ganglia and neurons*

The criteria were adapted from Swaminathan and Kapur<sup>1</sup>.

- All areas counted must be between circular and longitudinal layers of the muscularis externa.
- An area of dark brown perikaryal staining in a cell that contains a nucleus
  - Granular stain must cover the nucleus OR encircle at least 50% of circumference of the nucleus
  - AND at least some cytoplasmic granular brown staining must be present.
- Overlapping or continuous areas of dark brown staining, in the presence of two distinct nuclei and cell membranes, should be counted as two cell bodies.
- If there is any ambiguity about the presence of a nucleus, the cell should not be included.

The definition of a ganglion was a neural structure containing at least two neurons<sup>2</sup>.

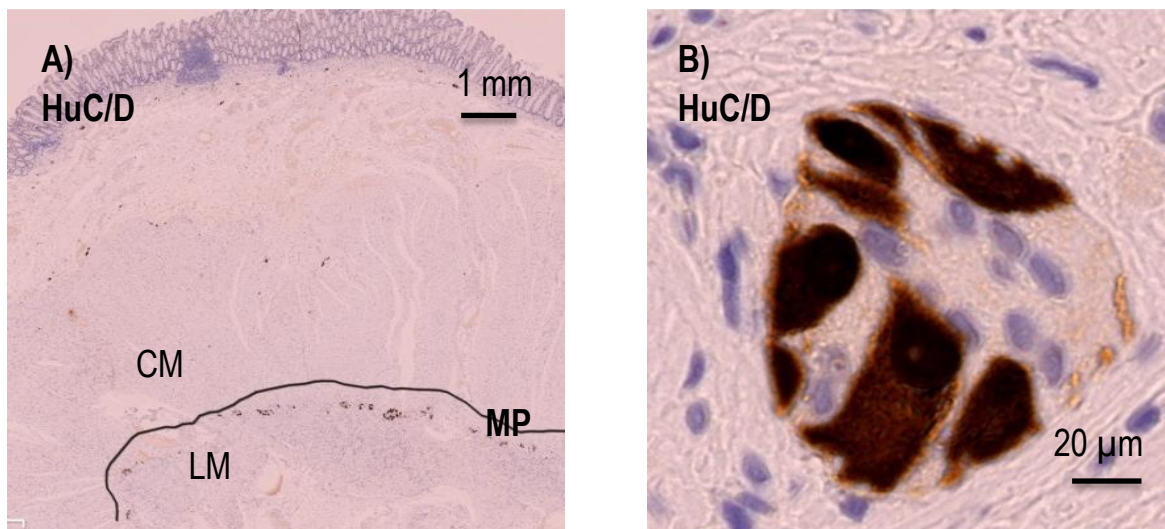
In all sections, a line was drawn along the myenteric plane between the circular and longitudinal muscles layers to measure the length of myenteric plexus, using the freehand draw function in the viewing software at low magnification (10-20x) (see Figure below). Two of the authors then identified and counted the neuron cell bodies and ganglia independently. The sections were assigned with codes to conceal the identity of the tissues, broken only for analyses of the results.

For myenteric ganglia counts, sections were stained with HuC/D and viewed at ~40x magnification. To quantify neuron cell bodies, sections were stained with HuC/D antibody and viewed at high magnification (60-80x). Similarly, subclasses of neuron cell bodies were counted using sections stained with anti-ChAT and anti-nNOS. In the block from each patient, multiple sections were used, at least 16  $\mu\text{m}$  apart, so at least 10 mm of myenteric plexus had been assessed for each stain, but usually more.

**Suppl. Figure 1: HuC/D immunostaining.**

- A) Section showing line drawn to measure myenteric plexus
- B) HuC/D immunolabelling of neurons in a myenteric ganglion

For quantification, ganglia & neuronal number expressed by length of myenteric plexus



**1.3. Data Analysis**

The total length of myenteric plexus, number of ganglion and number of ganglion cell bodies across the different sections were determined for each patient. Quantification of ganglia was expressed as the mean ( $\pm$  standard error of mean) number of ganglia per mm of the myenteric plexus, drawn as described above. Numbers of myenteric neurons were expressed as the mean ( $\pm$  standard error of mean) number of cell bodies per mm of myenteric plexus. The values determined by the two 'blinded' observers were averaged and % inter-rater differences [95% CI] analyzed using one sample Student's *t*-tests and proportional biases investigated using Bland-Altman plots.

**2. Density of PGP positive nerve fibres in circular and longitudinal muscle**

Sections were labelled using antibodies raised against PGP9.5 (Table).

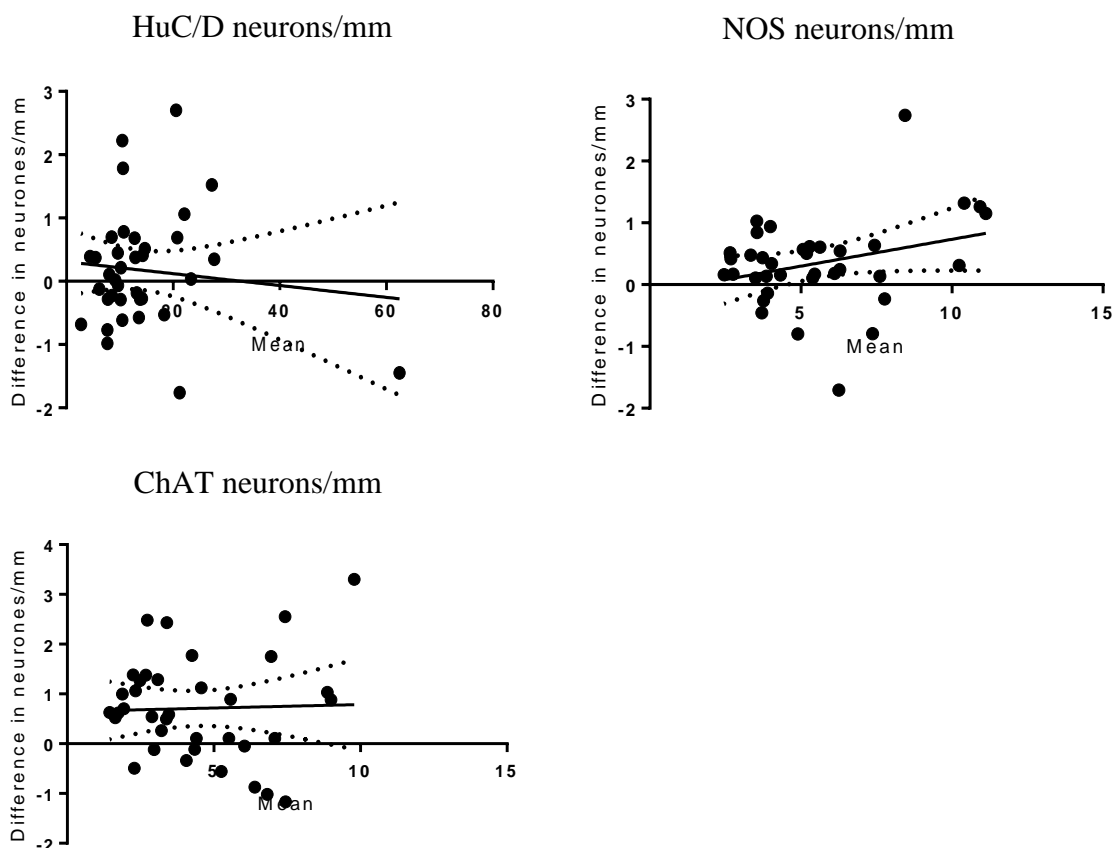
Three regions per section were investigated independently by two observers (circular muscle near the myenteric plexus, circular muscle close to the mucosa (deep circular muscle), and the longitudinal muscle) using NDP.view2 Viewing software: U12388-01 (Hamamatsu). Four non-sequential sections were analysed per patient. For each section, two 400 x 400

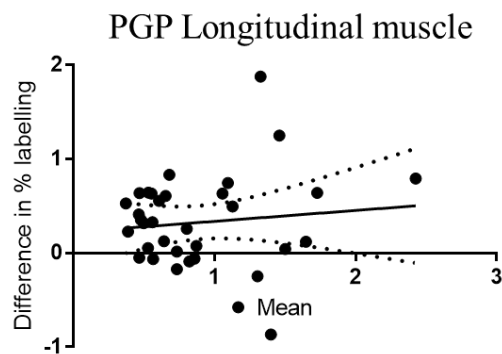
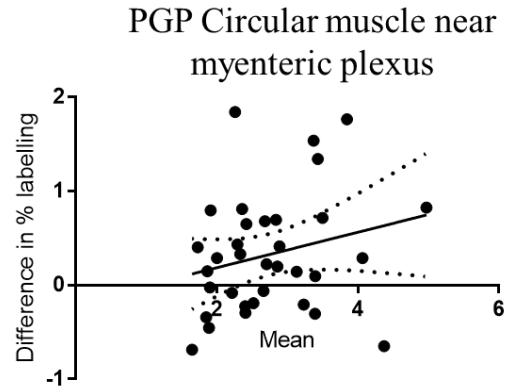
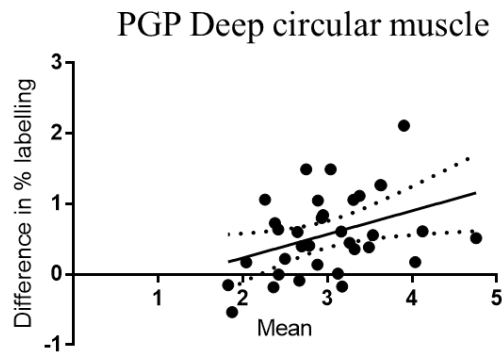
pixel boxes were captured at 10X magnification for each region. Images were exported from NDP viewer and cropped to 400 x 400 pixels in Image J (NIH).<sup>3</sup> For analysis of PGP9.5 staining, the images were converted to grayscale using the binary function in ImageJ. The contrast of the image was adjusted to illustrate PGP-positive fibres only without the smooth muscle cells, and the % staining was determined from the positive pixel labelling to indicate the density of PGP fibres in the respective muscle layer. The values, determined by the two blinded observers, were averaged for each patient. Group data were expressed as means  $\pm$  standard error of mean. Differences in PGP9.5 fibre density between the adult ascending and descending colon and between the two age groups were compared using Student's *t*-tests in GraphPad Prism 7.02;  $P < 0.05$  was considered statistically significant.

### Inter-rater differences in quantification of neurons

One of the two independent observers obtained significantly higher absolute counts for the number of ChAT positive and nNOS positive nerve cell bodies per mm of myenteric plexus and for the density of PGP positive nerve fibres in smooth muscles ( $P < 0.05$  each; one sample *t* test).

Bland Altman plots





Inter-rater differences were found to increase with the average counts (i.e. proportional bias) for the density of PGP staining in deep circular muscles.

Nevertheless, for all antibodies both observers identified the same statistically significant changes or trends in the elderly (Supplementary Tables 2 and 3). For example, in adult and elderly ascending colon the numbers of ChAT-positive neurons/mm increased from, respectively,  $2.5 \pm 0.3$  to  $5.4 \pm 0.6$  for Observer 1 ( $P=0.001$ ) and from  $2.2 \pm 0.3$  to  $4.7 \pm 0.8$  for Observer 2 ( $P=0.01$ ). Again, in adult and elderly colon, the staining for PGP9.5 in the deep circular muscle tended to be higher in the adult descending colon than the adult ascending and elderly descending colon for both observers. The discrepancies observed in this study were in the circular muscle near the myenteric plexus, where there was a significant decrease in staining in the elderly ascending compared to the adult ascending colon by observer 1 ( $3.0 \pm 0.2$ ,  $n = 7$  to  $2.2 \pm 0.1$ ,  $n = 8$ ;  $P = 0.003$ ), but no significant change in staining by observer 2 ( $2.3 \pm 0.2$ ,  $n = 7$  to  $2.0 \pm 0.1$ ,  $n = 8$ ;  $P = 0.24$ ) and in the longitudinal muscle there was a significant increase in staining observed in the adult descending colon compared to the adult ascending colon reported by observer 1 ( $1.4 \pm 0.2$ ,  $n = 10$  to  $0.7 \pm 0.05$ ,  $n = 7$ ;  $P = 0.03$ ), but not by observer 2 ( $0.8 \pm 0.2$ ,  $n = 10$  to  $0.40 \pm 0.1$ ,  $n = 7$ ;  $P = 0.10$ ).

Supplementary Table 2

Summary of cell bodies stained by antibodies for HuC/D, ChAT and nNOS per mm myenteric plexus in different regions of colon from patients of different age groups. The data are expressed as means  $\pm$  S.E.M. Differences between the two age groups and regions of colon were analysed by one-way ANOVA plus Sidak's test for multiple comparisons; \*  $P < 0.05$  (between age groups) and †  $P < 0.05$ , ††  $P < 0.01$  (between regions).

<b>Stain/region</b>	<b>Adult Ascending (n = 8)</b>	<b>Elderly Ascending (n = 9)</b>	<b>Adult Descending (n = 9)</b>	<b>Elderly Descending (n = 10)</b>
<i>Combined counts for both observers</i>				
HuC/D	7.0 $\pm$ 0.9	10.2 $\pm$ 0.9	22.9 $\pm$ 5.5††	15.7 $\pm$ 1.5
ChAT	2.4 $\pm$ 0.3	5.0 $\pm$ 0.6*	5.2 $\pm$ 0.8†	5.0 $\pm$ 0.8
NOS	3.8 $\pm$ 0.4	5.3 $\pm$ 0.8	6.6 $\pm$ 0.8	6.2 $\pm$ 0.8
<i>Observer 1</i>				
HuC/D	7.0 $\pm$ 0.9	10.4 $\pm$ 1.0	23.1 $\pm$ 5.4††	15.7 $\pm$ 1.4
ChAT	2.5 $\pm$ 0.3	5.4 $\pm$ 0.6*	5.7 $\pm$ 0.9†	5.3 $\pm$ 0.7
NOS	3.9 $\pm$ 0.4	5.4 $\pm$ 0.9	6.9 $\pm$ 0.9†	6.3 $\pm$ 0.8
<i>Observer 2</i>				
HuC/D	7.1 $\pm$ 0.9	10.0 $\pm$ 0.9	22.7 $\pm$ 5.6††	15.7 $\pm$ 1.5
ChAT	2.2 $\pm$ 0.3	4.7 $\pm$ 0.8	4.8 $\pm$ 0.8	4.7 $\pm$ 0.8
NOS	3.7 $\pm$ 0.4	5.1 $\pm$ 0.8	6.2 $\pm$ 0.8	6.2 $\pm$ 0.8

### Supplementary Table 3

Summary of staining by the PGP9.5 antibody in different areas of muscle in the colon from patients of different age groups. The data are expressed as means  $\pm$  S.E.M. Differences between the two age groups and regions of colon were analysed by 1 way ANOVA plus



Sidak's test for multiple comparisons; \*\* P < 0.01 (between age groups) and † P < 0.05, †† P < 0.01 (between regions).

<b>Age/region/ area</b>	<b>Adult Ascending (n = 7)</b>	<b>Elderly Ascending (n = 8)</b>	<b>Adult Descending (n = 10)</b>	<b>Elderly Descending (n = 9)</b>
<b><i>Combined counts for both observers</i></b>				
Deep Circular muscle	2.8 ± 0.2	2.5 ± 0.1	3.7 ± 0.2††	2.8 ± 0.2**
Circular muscle near myenteric plexus	2.7 ± 0.2	2.1 ± 0.1	3.2 ± 0.3	2.8 ± 0.2
Longitudinal muscle	0.5 ± 0.1	0.7 ± 0.1	1.1 ± 0.2†	1.1 ± 0.1
<b><i>Observer 1</i></b>				
Deep Circular muscle	3.1 ± 0.3	2.7 ± 0.2	4.1 ± 0.2†	3.0 ± 0.2**
Circular muscle near myenteric plexus	3.1 ± 0.2	2.2 ± 0.1	3.4 ± 0.3	2.8 ± 0.3
Longitudinal muscle	0.7 ± 0.05	0.9 ± 0.1	1.4 ± 0.2†	1.1 ± 0.2
<b><i>Observer 2</i></b>				
Deep Circular muscle	2.5 ± 0.2	2.3 ± 0.1	3.3 ± 0.2††	2.6 ± 0.1**
Circular muscle near myenteric	2.3 ± 0.2	2.0 ± 0.1	3.0 ± 0.3	2.8 ± 0.2

plexus

Longitudinal muscle	$0.4 \pm 0.1$	$0.6 \pm 0.1$	$0.8 \pm 0.2$	$1.0 \pm 0.2$
---------------------	---------------	---------------	---------------	---------------

## References

<sup>1</sup> Swaminathan M, Kapur RP. Counting myenteric ganglion cells in histologic sections: an empirical approach. *Hum Pathol* 2010;41:1097-108.

<sup>2</sup> Knowles CH, Veress B, Kapur RP, et al. Quantitation of cellular components of the enteric nervous system in the normal human gastrointestinal tract--report on behalf of the Gastro 2009 International Working Group. *Neurogastroenterol Motil* 2011;23:115-24.

<sup>3</sup> Schneider CA, Rasband WS, Eliceiri KW. NIH Image to ImageJ: 25 years of image analysis. *Nature Methods* 2012;9:671-5.